Thermal Imaging of Receptor-Activated Heat Production in Single Cells

Ofer Zohar,* Masayaki Ikeda,# Hiroyuki Shinagawa,# Hiroko Inoue,# Hiroshi Nakamura,# Danek Elbaum,§ Daniel L. Alkon,* and Tohru Yoshioka#

*Laboratory of Adaptive Systems, National Institute of Neurological Disorders and Stroke, Bethesda, Maryland 20892-4124 USA; #Department of Molecular Neurobiology, School of Human Science, Waseda University, Saitaima 359, Japan; and §Nenski Institute of Experimental Biology, PAN, Warsaw, Poland

ABSTRACT Changes in enthalpy (i.e., heat content) occur during the diverse intracellular chemical and biophysical interactions that take place in the life cycle of biological cells. Such changes have previously been measured for cell suspensions or cell-free biochemical extracts by using microcalorimetry, thermocouples, or pyroelectric films, all of which afford minimal spatial or temporal resolution. Here we present a novel thermal imaging method that combines both diffraction-limited spatial (~300 nm) and sampling-rate-limited time resolution, using the temperature-dependent phosphorescence intensity of the rare earth chelate Eu-TTA (europium (III) thenoyltrifluoro-acetonate). With this thermosensitive dye, we imaged intracellular heat waves evoked in Chinese hamster ovary cells after activation of the metabotropic m1-muscarinic receptor. Fast application of acetylcholine onto the cells evoked a biphasic heat wave that was blocked by atropine, and after a brief delay was followed by a calcium wave. Atropine applied by itself produced a monophasic heat wave in the cells, suggesting that its interactions with the receptor activate some intracellular metabolic pathways. The thermal imaging technique introduced here should provide new insights into cellular functions by resolving the location, kinetics, and quantity of intracellular heat production.

INTRODUCTION

The interactions of individual cells with their microenvironment lead to the activation of specific intracellular metabolic pathways. After activation of a metabolic pathway, sequential heat-producing interactions with distinct kinetics ensue. Microcalorimetry is the most established technique for studying metabolic heat that has been used to study various aspects of cellular activity. Microcalorimetry has been used to monitor the effect of drugs in general (Lonnbro and Wadso, 1991) and specific (Wang and Chang-Hwei, 1992) metabolic heats, the effect of immunomodulators on cellular activity (Faldt et al., 1982; Beezer et al., 1993), increased cellular activity in hyperthyroidism (Monti et al., 1987), the effect of second messengers on intracellular enzyme activity (Kodama et al., 1984), and the energetics of membranal Na^+-K^+ ATPase activity (Gruwel et al., 1995). Although microcalorimeters used for these studies have high thermal resolution, they have poor spatial and temporal resolution, and they are used to measure steady-state heat production of large numbers of reactants in suspension.

A few attempts have been made to measure the initial heat associated with action potential propagation in neuronal tissue by using either thermocouples (Abbot et al., 1958; Howarth et al., 1968) or pyroelectric films (Tasaki et al., 1989). This initial heat occurs within a fast (less than 0.5-s latency) biphasic (positive followed by negative) heat wave. In myelinated nerves, the peak of the positive heat wave was measured to be a few tens of μcal/g, whereas in nonmyelinated nerves it was <0.5 μcal/g (Keynes and Ritchie, 1970; Howarth et al., 1975; Tasaki and Byrne, 1992). Thermocouples and pyroelectric films have high temporal resolution but low spatial resolution, and the thermal conductivity between the tissue and the sensor is poor. Steady-state temperatures of cell suspension were also measured with fluorescent probes with ~1°C resolution (Chapman et al., 1995). Although m1 muscarinic receptor-ligand interaction and consequent second messenger activity were studied extensively (Felder et al., 1989; Lechleiter et al., 1991; Berridge, 1993), and in some cases the ligand-receptor Van Hoff's heats were calculated from the temperature effects on the binding constants (Gies et al., 1987), no direct measurement of heat derived from in situ ligand-receptor interactions has been attempted in this or any metabolic system.

We present here a novel thermal imaging method that images for the first time metabolic heat signals generated by m1-muscarinic ligand-receptor interactions in single Chinese hamster ovary (CHO) cells that were genetically manipulated to express the receptors (Buck and Fraser, 1990) (CHM). The technique combines both diffraction-limited spatial (~300 nm) and sampling-rate-limited time resolution, using the temperature-dependent phosphorescence intensity of the rare earth chelate europium (III) thenoyltrifluoro-acetonate (Eu-TTA). Eu-TTA has previously been used for noncontact failure analysis of integrated circuits covered by thin films of the dye mixed with liquid crystals (Kolodner and Tyson, 1982). Defective electronic connections that have higher impedance produce more heat and thus can be imaged with a temperature resolution of a few m°C (Kolodner and Tyson, 1983; Barton, 1994). Excitation of the TTA ligand is transferred via its triplet electronic

Received for publication 8 May 1997 and in final form 22 October 1997.

Address reprint requests to Dr. Ofer Zohar, Laboratory of Adaptive Systems, National Institute of Neurological Disorders and Stroke, 36 Convent Drive MSC 4124, Bethesda, MD 20892-4124. Tel.: 301-496-3662; Fax: 301-402-2281; E-mail: zohar@codon.nih.gov.

0006-3495/98/01/82/08 $2.00

level to the $5d_o$ level of the Eu^{3+} ion, which in turn fluoresces in a narrow band around 614 nm (Crosby et al., 1961; Winston et al., 1963). At room temperature, the quantum efficiency of Eu-TTA phosphorescence declines rapidly with increasing temperatures because of competition with nonradiative processes and coupling, through molecular vibrations between the electronic energy levels and the environment (Bhaumik, 1964).

In this study we used the thermosensitive dye Eu-TTA that was integrated within CHO cell membranes (CHO-EuTTA) to image intracellular heat waves evoked at room temperature, after a brief activation of m1 muscarinic receptors by acetylcholine (ACh). In these cells, ACh application activates typical calcium waves that have a much longer latency and duration than a typical heat wave. No measurable pH change was associated with ACh application onto CHM cells. The heat response was completely blocked by preincubating the cells in atropine, and application of the vehicle alone did not produce any phosphorescence signal. Brief application of atropine did generate a monophasic heat wave in the cells. This result is consistent with several previous studies that suggested that atropine activate some intracellular metabolic pathways (Horn et al., 1991a). All of the patterns of heat generation described above were confirmed by an independent microcalorimetric study (Zohar et al., manuscript in preparation).

MATERIALS AND METHODS

Stained liposome preparation

Liposomes with Eu-TTA embedded within their membranes were prepared by diluting 300 μl of L-α-lecithin (Sigma, St. Louis, MO; 20 mg/ml) and 1035 μl of Eu-TTA (ACROS Organics, Pittsburgh, PA; 100 mM) in chloroform in a ball-shaped flask. The chloroform was evaporated slowly under low air pressure while the flask was rotated continuously. In this way a thin layer of L-α-lecithin mixed with Eu-TTA was formed on the glass walls. Three milliliters of buffered saline solution (BSS) (130 mM NaCl, 5.4 mM KCl, 2 mM $CaCl_2$, 1 mM $MgCl_2$, 5.5 mM D-glucose, 10 mM HEPES-Na, pH 7.4; Sigma) was then added to the flask, the mixture was vortexed for 10 min to form liposomes and transferred to 3-ml quartz cuvettes, and its luminescence was measured in a temperature-controlled spectrofluorometer (Spex 3200, Edison, NJ; emission: 614 nm, excitation: dimethyl sulfoxide (DMSO), 359 nm; BSS and liposomes, 372 nm; CHO cells, 363 nm). Before each measurement, the temperature of the mixture was allowed to equilibrate in the spectrofluorometer for 10 min. pH dependency of the dye in stained liposomes was measured at room temperature (22°C).

Cells: culture and experimental

CHO cells were cultured in a high-glucose minimum essential medium with 10% fetal bovine serum solution (α-medium; Gibco BRL, Grand Island, NY). For the imaging experiments, cells were grown on 35-mm glass-bottomed petri dishes at 37°C, and before the experiment the culture medium was replaced with BSS. For the spectral analysis, cells were grown in plastic flasks (Nunc 75 cm^2), and before the experiment were detached by incubating them for 10 min in phosphate-buffered saline (Gibco BRL) containing 1 mM EDTA, centrifuged for 5 min at 1000 RPM, and washed with BSS. Staining the cells (either in the petri dish or in suspension) with Eu-TTA was done by adding 50 μM Eu-TTA (from a 10 mM stock dissolved in DMSO) to 3 ml of BSS and allowing the cells to incubate for 30 min at room temperature. The cells were then washed three times with BSS.

Thermal imaging; technique and image analysis

Heat evoked in the cells was recorded with a cooled CCD camera (256 × 256 pixel array; Hamamatsu 4880, Hamamatsu, Japan) connected to an inverted microscope (Axiovert 405M; Zeiss). Data were collected on line by using a 40× 1.2 NA Zeiss objective and were analyzed later on a Pentium computer (Dell 133 MHz) using the Argus 50 system (Hamamatsu). CHO-EuTTA and CHM-EuTTA were excited by applying 100-ms UV light flashes (mercury 100 W) every second (excitation: 365 ± 30 nm bandpass; dichroic: 480 nm; emission: 510 nm long pass; Omega Optical, Battleboro, VT). Images were collected at 1.1-s intervals. During the experiments cells were continuously perfused with BSS (2 ml/min). Drugs (50 μl) were pressure applied (100 ms) at a distance of ~200 μm upstream of the recording area.

Dependence of the phosphorescence intensity of CHO-EuTTA on external temperature was imaged under temperature-controlled perfusion. The temperature of the perfused BSS was reduced to 15°C for 70 s (as monitored by a thermocouple in the recording dish), after which the BSS temperature was allowed to reach 25°C (by turning off the temperature-controlled water bath). Finally, the BSS temperature was cooled back to 15°C.

The optical recordings of Eu-TTA luminescence were affected by both thermobleaching and photobleaching, and each pixel had a different initial intensity. To normalize the images for intensity, each frame was divided by the first frame in the series on a pixel-to-pixel basis. Photobleaching caused the Eu-TTA phosphorescence signal to decay in an exponential manner. The temperature effects on the luminescence signals were exposed differently in the external temperature experiment (Fig. 1, *E–F*) and in the physiological experiments (Figs. 2, *A–C*, and 4, *A–C*). In the external temperature experiments the exponents describing the decay in the first 15°C phase were calculated and then "peeled" off the entire recording. In this way the first 15°C phase appeared as a straight line, and the rest of the curve thus represented the external temperature effects on the CHM-EuTTA cells.

In the physiological experiments a pretreatment baseline was collected before the pressure application of the chosen substance in each experiment. With this baseline the exponential decay constant of the photobleaching was calculated on a pixel-to-pixel basis and subtracted mathematically from the entire record (these mathematical processes, i.e., ratioing and subtracting, were performed automatically by the Argus 50 system). As a result, the baseline recordings before the treatment appeared as a straight line, and the temperature effects on emission intensity became apparent. In both types of experiment, the equation $1 - f(x)$ was employed for each calculated data point, so as to associate higher values with positive heat production.

Calcium imaging

The intracellular calcium response to an ACh (RBI, Natick, MA) puff at 22°C or 12°C was measured by conventional techniques. Before the experiment, the cells were incubated for 30 min in 6 μM Fura-2-AM (Molecular Probes, Eugene, OR), washed with BSS, and then incubated for additional 20 min at 37°C to inactivate the free Fura-2-AM. Intracellular calcium concentrations were estimated from the ratios of emission intensities excited by consecutive pairs (2 s) of 340/380-nm light pulses (dichroic: 430 nm; emission: 510 nm long pass).

pH imaging

Before the experiment cells were incubated for 30 min in 3 μM 2′,7′-bis-(2-carboxyethyl)-5-(and-6)-carboxyfluorescein, acetoxymethyl ester (BCECF-AM) or carboxy SNARF-1 (Molecular Probes), washed with BSS, and then incubated for an additional 10 min at 37°C to inactivate the free esters. pH was estimated from the ratio of emission intensity excited

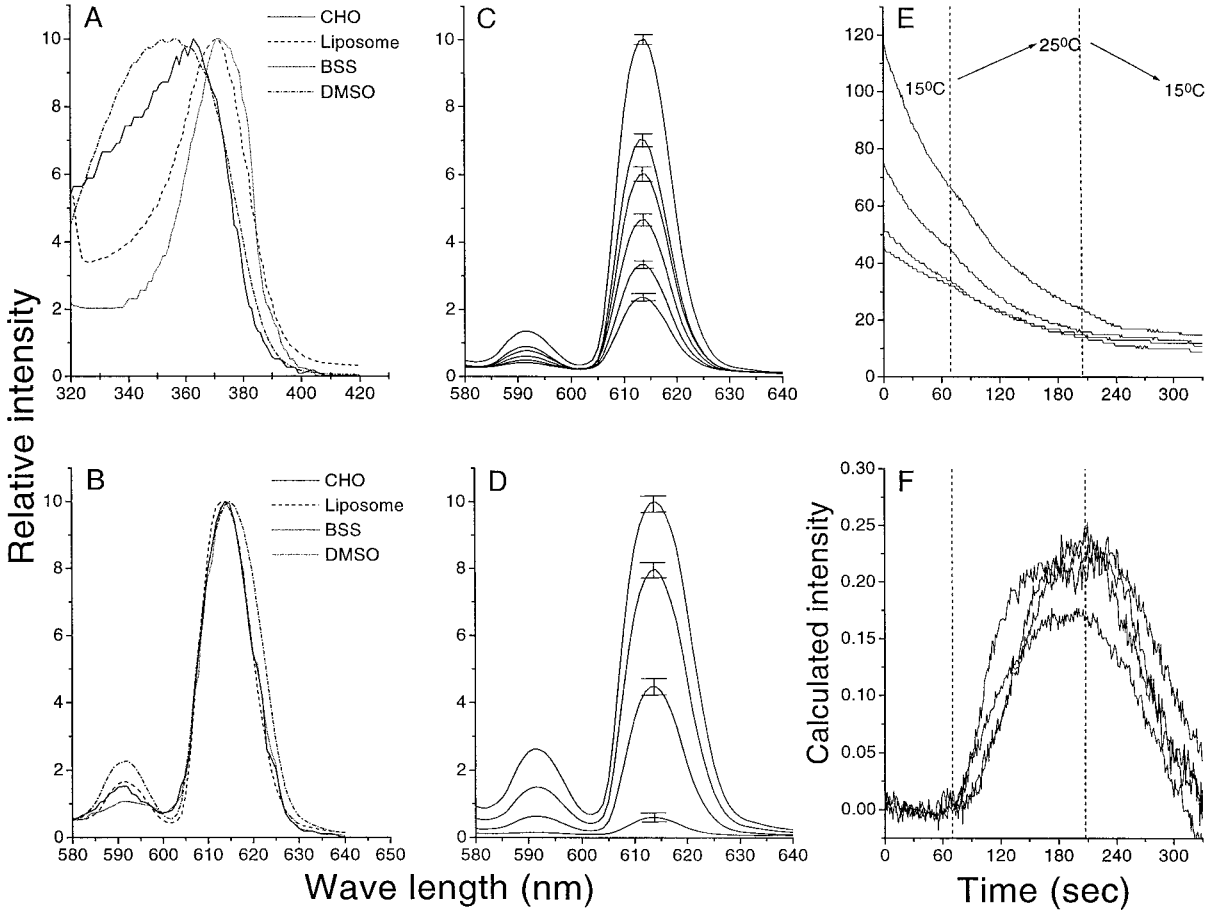

FIGURE 1 Effect of chemical environment on the spectral properties of the thermosensitive dye Eu-TTA (*A* and *B*) and on its emission intensity (*C–F*). (*A*) Excitation spectra of the dye integrated with CHO cell membrane, integrated into liposomal membranes, and dissolved in BSS or in DMSO. All peaks were normalized to 10 (emission 615 nm). (*B*) Emission spectra of the dye under the same conditions as in *A*. All emission peaks were normalized to 10 (excitation according to the peaks shown at *A*). (*C*) Dependence of Eu-TTA emission intensity on temperature while integrated in liposomal membranes. The temperature was varied between 15°C and 40°C (*top to bottom*) at 5°C intervals (pH 7.4). Each curve represents an average of a steady-state measurement ($n = 6$; for clarity, SEM is shown only at the peak of each curve). (*D*) Dependence of Eu-TTA emission intensity on pH when the dye was integrated into liposomal membranes. The pH was varied between 5 and 8 (*top to bottom*) in 1 pH unit intervals (22°C). Each curve represents an average of steady-state measurements ($n = 6$; for clarity, SEM is shown only at the peak of each curve). (*E*) Optical recordings of luminescence intensity change in CHO-EuTTA, as a result of changing the bath perfusion temperature. Each line represents optical recording from a single cell. (*F*) The calculated intensity ratio of the recordings in Fig. 1 *E*. The initial recordings at 15°C are clearly followed by temperature effects on emission intensity.

by consecutive pairs (2 s) of 450/490-nm light pulses. Standards for the pH imaging were obtained from BCECF-labeled cells that were pretreated by the H^+ ionophore nigericin (20 mM; Sigma) and placed in a buffer containing 130 mM KCl and 20 mM HEPES, at pH values between 6.3 and 8.0.

RESULTS

We found Eu-TTA to be hydrophobic, and it readily stained biological membranes. Moreover, when in aqueous solutions the luminescence of Eu-TTA faded rapidly, in lipophilic environments it was more stable. The dye was excited by a wide range of wavelengths peaking around 370 nm (Fig. 1 *A*) and emitted a narrow bright red band (Fig. 1 *B*). (In Fig. 1, *A* and *B*, all peaks were normalized to 10, and the rest of the data points were calculated as a proportion of the peak value.) The excitation spectrum varied slightly in different media. Excitation peaked at 357 nm (bandwidth at half-peak (BWHP) = 56 nm) in DMSO (50 μM Eu-TTA), at 363 nm (BWHP = 58 nm) in CHO-EuTTA, at 372 nm (BWHP = 33 nm) in liposomes, and at 372 nm (BWHP = 28 nm) when dissolved in BSS. The emission spectra were not sensitive to the chemical environment, and showed a small peak at 592 nm and a large narrow peak at 614 nm (BWHP = 15 nm).

While Eu-TTA was integrated in liposomal membranes, the emission intensity of the Eu-TTA luminescence was found to be temperature dependent between 15°C and 40°C (pH 7.4; the temperature was varied in 5°C intervals) (Fig. 1 *C*). Each curve represents an average of a steady-state measurement ($n = 6$; for clarity, SEM is shown only at the peak of each curve). The peak of the strongest emission (15°C) was normalized to 10, and then the rest of the measurements (20–40°C) were calculated as a proportion

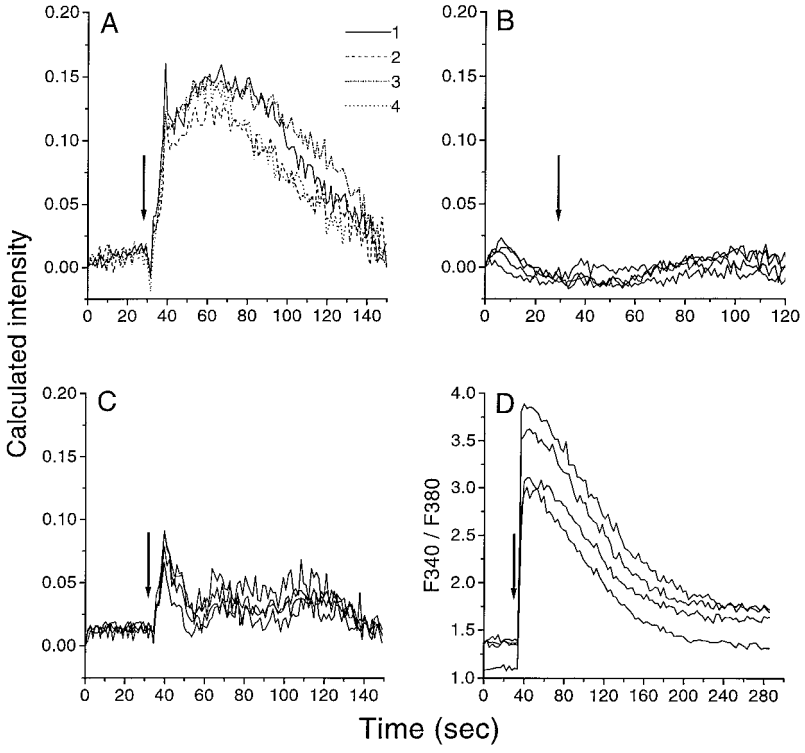

FIGURE 2 Thermogenesis and intracellular calcium concentration changes of -EuTTA cells in response to a brief application of ACh. In *A–C* the calculated intensity ratio is presented. In all figures each line represents one cell. Arrows denote puff timing; note the different time scales. (*A*) Optical recordings of ACh-evoked thermogenesis at 22°C in the cells. The recordings were taken from the cells marked in the top left frame of Fig. 3; the same number coding is used. (*B*) Atropine blocked the ACh-evoked thermogenic responses of the cells. (*C*) Optical recording of ACh-evoked thermogenesis at 12°C. All conditions and treatment were the same as in *A*. (*D*) Intracellular calcium response to ACh puff at 22°C.

of the emission peaks for each measurement point. The emission diminished by ~2% per degree Celsius between 20°C and 40°C, and by ~6% between 15°C and 20°C. Emission of Eu-TTA incorporated into liposomal membrane was sensitive to pH change between 5 and 8 as well (22°C). Each curve represents an average of steady-state measurements ($n = 6$; for clarity, SEM is shown only at the peak of each curve). Data were normalized as described above for the peak at pH 5. Between pH 5 and 6 emission diminished by 20%, and between pH 6 and 8 it diminished by ~40% per pH unit. Dependence of CHO-EuTTA on external temperature change could be monitored by our imaging system. When CHO-EuTTA was radiated by pulsed UV light, the dye luminescence photobleached, and the photobleaching described an exponential decay (Fig. 1 *E*). With increasing temperatures, the emission intensity bleached more quickly. The temperature dependence of these thermobleaching effects followed its own distinct decay, which was apparent after the mathematical manipulations of the recordings (Fig. 1 *F*). The initial recordings at 15°C are clearly followed by temperature effects on emission intensity. No apparent toxicity of Eu-TTA to biological cells was observed in this study. Stained CHO cells did not detach from their coverslips, even after several hours, nor did their morphology change. Preliminary electrophysiological studies also showed no change in the properties of stained neurons. Further investigations will have to be conducted to determine the LD_{50} of the dye in different tissues.

Pressure-ejected acetylcholine (ACh) puffed onto cells elicited a change in phosphorescence that most probably derived from the heat produced by the cells. Expression of the receptor was confirmed by m1-type receptor-specific antibodies. At 22°C the ACh puff evoked a triphasic temperature-dependent fluorescent signal in many of the cells ($n = 126$; Fig. 2 *A*). (Imaging of the progressive heat wave in the cells is presented in Fig. 3.) The first phase was a fast cooling wave that lasted ~2.5 s. This cooling is most probably the endothermic heat of dilution of ACh in the BSS. Immediately after the cooling phase, two exothermic phases (fast and slower) were generated by the cells. The fast heat wave lasted for ~2 s, whereas the slow wave lasted for ~110 s. Both waves peaked at ~0.15 of the calculated signal. The complete kinetics of the signals could not be quantitatively resolved by our experimental conditions, which were limited by the ~1-s sampling rate of the cooled CCD camera. Atropine (0.5 mM) added to the dish before the experiment blocked the ACh-evoked heat response in these cells (Fig. 2 *B*). The peak of the thermogenic response elicited at 12°C by the ACh puff was half of the one elicited at 22°C; the signal was monophasic and lasted only ~15 s ($n = 126$; Fig. 2 *C*). A typical intracellular calcium wave generated by these cells in response to ACh at 22°C started ~4 s after the puff and lasted for ~3 min ($n = 126$: Fig. 2 *D*). At 12°C, on the other hand, no calcium response could be evoked by puffing ACh onto the cells ($n = 126$; data not shown). One important cellular consequence of the m1 muscarinic receptor activation is release of calcium from intracellular stores via the IP_3 pathway (Berridge, 1993). The correlation between the appearance of the calcium wave (Fig. 2 *D*) and the thermogenic response at both temperatures (12°C and 22°C; Fig. 2, *A* and *C*) suggests that some components of the m1 muscarinic signal transduction

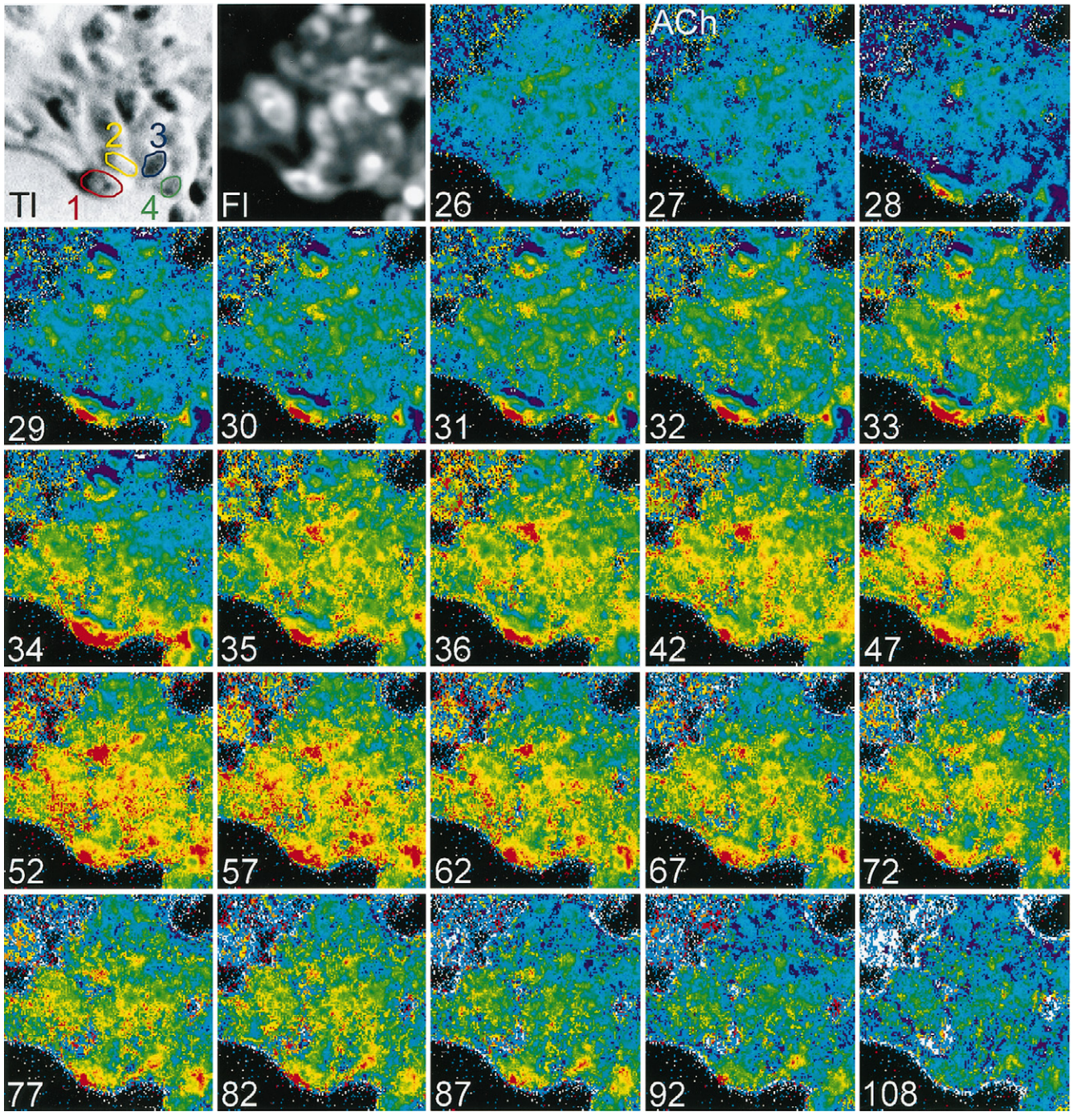

FIGURE 3 Thermal imaging of the heat wave evoked in a cluster of -EuTTA cells after a puff of ACh. The montage is constructed from a transmitted light image (TI), a luminescence image (FI), and consecutive pseudo-color images taken before and after the ACh application. The pseudo-color images are color-coded from blue through green and yellow to red (blue represents the highest gray level, i.e., colder areas, and red represents the lowest grey level, i.e., warmer areas). The numbers on the images are the frame numbers (frame interval ~1 s). Frame 26 presents the prepuff images; the ACh puff was given in frame 27, followed by nine consecutive frames (28–36); thereafter, frames are presented at intervals of ~5 s. Each frame was manipulated mathematically on a pixel-by-pixel basis. Immediately after the ACh application, an initial decrease of heat (frame 28) was indicated by increasing "blue" in the image. In succeeding frames (29–57) local heat generation was indicated in some cells by increased "red" in the image, which decayed thereafter.

pathway may be involved in the observed heat production. On the other hand, it is possible that the CHO cellular membranae shows a sol/gel phase transition between these temperatures, with a phosphorescence signal change as a consequence.

Surprisingly, atropine (a muscarinic receptor antagonist) puffed onto the cells elicited a monophasic exothermic heat signal from the cells. At 22°C, atropine generated a heat wave that lasted for ~90 s and peaked at 0.8 of the calculated signal (Fig. 4 *A*), whereas at 12°C the heat wave lasted

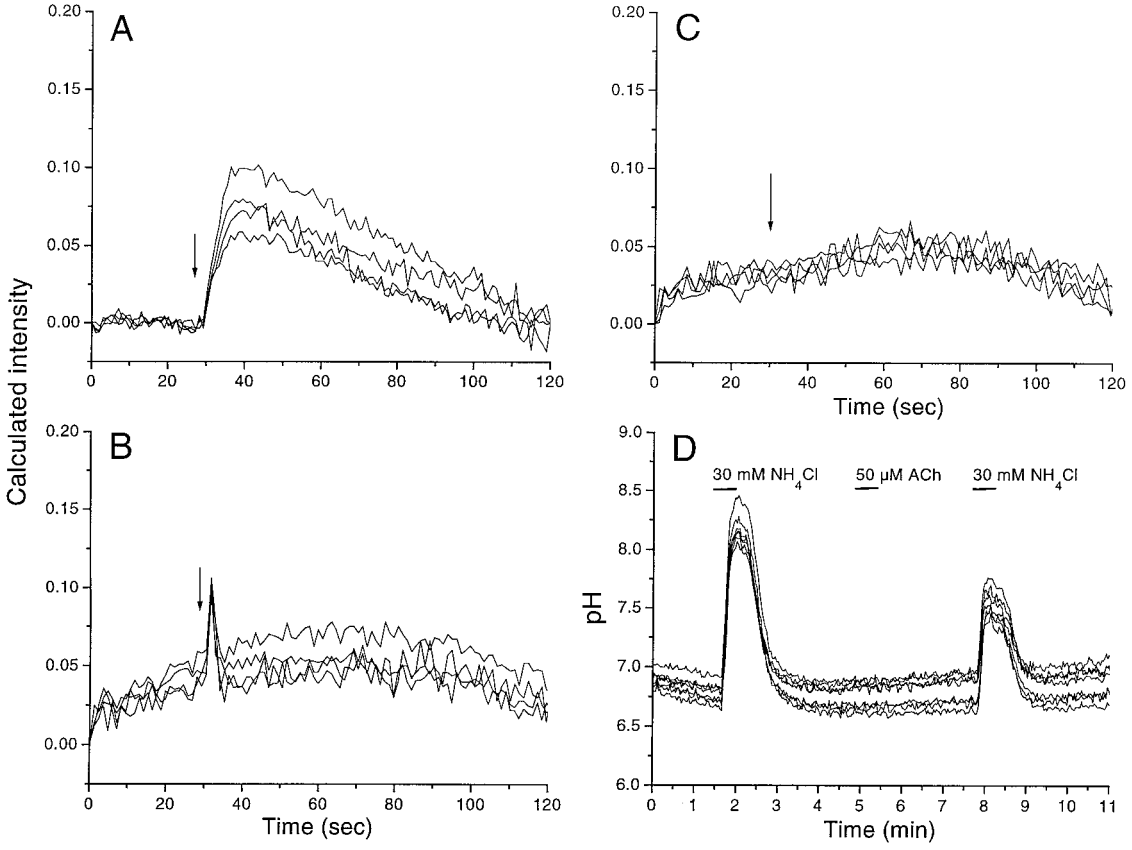

FIGURE 4 Optical recordings of different responses of -EuTTA cells to ligand application. In *A–C*, the calculated intensity ratio is presented. In all figures each line represents one cell. Arrows denote puff timing. Note the different time scales. (*A*) Optical recordings of atropine-evoked thermogenesis in the cells. (*B*) Atropine-induced thermogenesis at 12°C in the cells. (*C*) BSS puffed onto the -EuTTA cells at 22°C did not produce a fluorescence signal. (*D*) Optical recordings of the intracellular pH change in the cells after a 30-s bath application of either NH_4Cl or ACh at 22°C, as imaged with the pH-sensitive dye BCECF.

for ~4 s and peaked at 0.5 of the calculated signal (Fig. 4 *B*). The appearance of this heat wave suggests that in addition to its effect as a classical receptor blocker, atropine activates heat-generating pathways in the cells.

ACh puffs applied to normal CHO-EuTTA that do not express the muscarinic receptor (data not shown) or the vehicle alone puffed onto CHM-EuTTA cells did not elicit any fluorescent signal with a distinct time course at either temperature (Fig. 4 *C*). Optical recordings of the intracellular pH change in cells after a 30-s bath application of either ammonium chloride (30 mM NH_4Cl) or ACh (50 μM) at 22°C were imaged with the pH-sensitive dye BCECF (Fig. 4 *D*). Whereas the cells showed a marked change of ~1.5 pH units in response to the NH_4Cl application (applied twice), no detectable change was produced by the application of ACh. Optical recordings conducted with the pH-sensitive dye carboxy SNARF-1 yielded similar results, although they were somewhat attenuated under the same experimental protocol (data not shown). Furthermore, no pH change could be detected with a pH electrode (Corning, Corning, NY) upon the addition of ACh (0.5 mM) to a large number of CHM cells (10^6 in 3 ml).

Consistent with the results presented above, a microcalorimetric study showed reliably enhanced exothermic responses to ACh by cells, as compared to responses of normal CHO cells (n = 8; Zohar et al., manuscript in preparation). These direct measurements independently confirm, albeit with less spatial and temporal resolution, that the ACh-evoked change in luminescence intensity of Eu-TTA integrated within the cell membranes is associated with heat production.

DISCUSSION

In this study we show that activation of the metabotropic m1 muscarinic receptors can generate intracellular heat production. This heat generation can be monitored by Eu-TTA phosphorescence. The heat responses are most likely the result of biochemical metabolism in the cells and not the result of noncovalent binding and/or dissociation. The prolonged time course (2–3 min) of the ligand-activated luminescence signal was comparable to the duration of heat production measured by microcalorimetry (Zohar et al., manuscript in preparation), and started (Fig. 2 *A*) a few seconds earlier and was shorter than the intracellular calcium elevation (Fig. 2 *D*). The heat generated by ACh receptor-enriched membrane vesicles prepared from *Tor-*

pedo electric organ showed a similar time course of ~2 min in response to ACh (Wang and Chang-Hwei, 1992). On the other hand, the kinetics of agonist binding to ACh receptor is faster than 1 s (Heidmann et al., 1983; Niu et al., 1996). Furthermore, calculations of Van't Hoff enthalpy for muscarinic agonist-membrane binding was estimated to generate undetectably low heat levels (e.g., 40 ± 14 kcal (mol cell)$^{-1}$; Waelbroeck et al., 1985). Therefore, the observed responses in this study are, to our knowledge, most likely the first examples of receptor-activated metabolic heat generation demonstrated in single cells.

Once integrated with the liposomal membrane, the dye also showed intensity changes reciprocal to pH changes at room temperature. Under our experimental conditions we could not find any pH change associated with ACh application onto the CHM cells, either by using pH sensitive dyes or by using a pH electrode to measure the pH of large number of cells. Moreover, steady-state application of carbachol (ACh agonist) results in acidification of CHM cells (Baxter et al., 1994); the expected change in the Eu-TTA phosphorescence signal upon such acidification would have been in the direction opposite than observed here. However, for other systems and experimental conditions, this might not be the case. The Eu-TTA molecule easily loses its excited electron to the microenvironment upon temperature change (Bhaumik, 1964), so it is possible that a more significant pH change may alter the time an excited triplet electron would spend in the $5d_o$ orbital, thus changing its probability of being lost to the environment.

The signal transduction pathway of m1 muscarinic receptors has been studied extensively (Lambert et al., 1992; Brann et al., 1993; Felder, 1995). In this pathway phospholipase C (PLC) is activated by agonist binding to the receptor via a guanine nucleotide binding protein (G protein) and hydrolyzed by phosphatidylinositol-4,5-bisphosphate (PIP_2) into inositol-1,4,5-trisphosphate (IP_3) and diacylglycerol (DAG). IP_3 induces calcium ion release from intracellular stores, which in turn activates various Ca^{2+}-dependent metabolic processes and ATPases (Berridge, 1993). DAG activates protein kinase C (PKC), which, in turn, activates a wide range of metabolic processes in the cytosol and the nucleolus (Nishizuka, 1992, 1995). After the binding of the agonist to the receptor, the membrane-bound G protein and PKC are activated, and then, in turn, the intracellular metabolic pathways are activated. The biphasic heat wave evoked by ACh application on the m1 receptors in this study is consistent with the signal transduction pathway described above. It is possible that the activation of the membrane-associated G proteins and PKC is producing the fast initial heat wave, and the subsequent slow heat wave is produced by the intracellular metabolic events activated by IP_3 and PKC (Fig. 2 *A*). Moreover, close examination of the images presented in Fig. 3 (frames 29–36) shows that first the heat is produced at defined intracellular areas, and then heat production spreads to other sections of the cell. This suggests that these areas are the location where the first chemical reactions take place.

Interestingly, brief application of atropine alone produced a large monophasic heat wave that lasted ~90 s. Few studies had suggested that atropine is a partial agonist rather than a simple antagonist (Horn et al., 1991a,b). Using direct activation of the G proteins in cells rather than activating the m1 receptor, it was shown that atropine decreased intracellular Ca^{2+} elevation. This suggests that atropine is acting as a partial agonist and is affecting some chemical interactions within the cell, and not just blocking the m1 muscarinic receptor by simple binding. Our results support this finding.

Because Eu-TTA is integrated in cellular membranes, the thermal conductivity of membrane-associated and intracellular heat-generating interactions is very high. The exothermic heat waves evoked by receptor-agonist interaction, imaged here in single cells, suggest the possibility of measuring other enthalpy changes of biological molecules (Yoshioka and Suzuki, 1989). Imaging these heat changes may add to our understanding of other intracellular reactions (Kodama et al., 1984), such as receptor-effector coupling (St. Hilaire et al., 1994), ionic pumps (Gruwel et al., 1995), antigen-antibody interactions (Beezer et al., 1993), conformational changes of molecules (Wintrode et al., 1994), and perhaps ionic current flow. Furthermore, the technique may help us determine the mechanism of reactions responsible for sequential biochemical pathways, for example, production of second messengers within and between distinct intra- and intercellular compartments.

We thank Drs. M. Berridge, B. G. Schreurs, and M. Segal for comments and critical reading of the manuscript; Dr. H. Agmon-Snir for helping with the imaging; and Dr. P. D. Ross for his help with the microcalorimetry.

This work was supported in part by grant-in-aid 07279105 for Scientific Research on Priority Areas on Functional Development of Neural Circuits, the Ministry of Education, Science, Sports and Culture of Japan, and by the Research for the Future Program of the Japanese Society for the Promotion of Science.

REFERENCES

Abbot, B. C., A. V. Hill, and J. V. Howarth. 1958. The positive and negative heat production associated with a single impulse. *Proc. R. Soc. Lond. B.* 148:149–187.

Barton, D. L. 1994. Fluorescent microthermographic imaging. *Proc. Int. Symp. Test. Failure Anal.* 20:13–18.

Baxter, G. T., M. L. Young, D. L. Miller, and J. C. Owicki. 1994. Using microphysiometry to study the pharmacology of exogenously expressed m1 and m3 muscarinic receptors. *Life Sci.* 55:573–583.

Beezer, A. E., J. Navratil, A. Fiserova, and M. Pospisil. 1993. Different immunomodulator regulated patterns of effector target cell interactions: a novel application of microcalorimetry. *Microbios.* 73:205–213.

Berridge, M. J. 1993. Inositol trisphosphate and calcium signaling. *Nature*. 361:315–325.

Bhaumik, M. L. 1964. Quenching and temperature dependence of fluorescence in rare earth chelates. *J. Chem. Phys.* 40:3711–3715.

Brann, M. K., J. Ellis, H. Jorgensen, D. Hill-Eubanks, and S. V. P. Jones. 1993. Muscarinic acetylcholine receptor subtypes: localization and structure/function. *Prog. Brain Res.* 98:121–127.

Buck, M. A., and C. M. Fraser. 1990. Muscarinic acetylcholine receptor subtypes which selectively couple to phospholipase C: pharmacological and biochemical properties. *Biochem. Biophys. Res. Commun.* 173: 666–672.

Chapman, C. F., Y. Liu, G. J. Sonek, and B. J. Tromberg. 1995. The use of exogenous fluorescent probes for temperature measurements in single living cells. *Photochem. Photobiol.* 62:416–425.

Crosby, G. A., R. E. Whan, and R. M. Alire. 1961. Intramolecular energy transfer in rare earth chelates. Role of the triplet state. *J. Chem. Phys.* 34:743–748.

Faldt, R. J., J. Ankerst, M. Monti, and I. Wadso. 1982. Heat production in different populations of human blood cells exposed to immune complexes in vitro: the importance of the Fc parts of immunoglobulins and the influence of active complement. *Immunology.* 46:189–192.

Felder, C. C. 1995. Muscarinic acetylcholine receptors: signal transduction through multiple effectors. *FASEB J.* 9:619–625.

Felder, C. C., R. Y. Kanterman, A. L. Ma, and J. Axelrod. 1989. A transfected m1 muscarinic acetylcholine receptor stimulates adenylate cyclase via phosphatidylinositol hydrolysis. *J. Biol. Chem.* 264: 20356–20362.

Gies, J. P., B. Ilien, and Y. Landry. 1987. Temperature-dependence and heterogeneity of muscarinic agonist and antagonist binding. *Biochem. Pharmacol.* 36:2589–2597.

Gruwel, M. L. H., C. Alves, and J. Schrader. 1995. Na^+-K^+-ATPase in endothelial cell energetics: ^{23}Na nuclear magnetic resonance and calorimetry study. *Am. J. Physiol.* 268:H351–H358.

Heidmann, T., J. Bernhardt, E. Neumann, and J. P. Changeux. 1983. Rapid kinetics of agonist binding and permeability response analyzed in parallel on acetylcholine receptor rich membranes from *Torpedo marmorata. Biochemistry.* 22:5452–5459.

Horn, V. J., I. S. Ambudkar, and B. J. Baum. 1991a. High affinity quinuclidinyl benzilate binding to rat parotid membranes requires muscarinic receptor G protein interaction. *FEBS Lett.* 282:289–292.

Horn, V. J., B. J. Baum, and I. S. Ambudkar. 1991b. Muscarinic receptor agonist effects in parotid acini and cells: evidence of G protein involvement. *Biochem. Biophys. Res. Commun.* 177:784–789.

Howarth, J. V., R. D. Keynes, and J. M. Ritchie. 1968. The origin of the initial heat associated with a single impulse in mammalian non myelinated nerve fibers. *J. Physiol. (Lond.).* 194:745–793.

Howarth, J. V., R. D. Keynes, J. M. Ritchie, and A. Von Muralt. 1975. The heat production associated with the passage of a single impulse in pike olfactory nerve fibers. *J. Physiol. (Lond.).* 249:349–368.

Keynes, R. D., and J. M. Ritchie. 1970. The initial heat production of amphibian myelinated nerve fibers. *J. Physiol. (Lond.).* 210:29–30.

Kodama, T., N. Kurebayashi, H. Harafuji, and Y. Ogawa. 1984. Calorimetric studies of the mechanism of the Ca^{2+}-ATPase reaction of sarcoplasmic reticulum. *J. Biochem.* 96:887–894.

Kolodner, P., and A. Tyson, 1982. Microscopic fluorescent imaging of surface temperature profiles with 0.01°C resolution. *Appl. Phys. Lett.* 40:782–784.

Kolodner, P., and A. Tyson. 1983. Remote thermal imaging with 0.7-micron spatial resolution using temperature-dependent fluorescent thin films. *Appl. Phys. Lett.* 42:117–119.

Lambert, D. G., N. T. Burford., and S. R. Nahorski. 1992. Muscarinic receptor subtypes: inositol phosphates and intracellular calcium. *Biochem. Soc. Trans.* 20:130–135.

Lechleiter, J. S., S. Girard, and E. Peralta. 1991. Subcellular pattern of calcium release determined by G protein-specific residues of muscarinic receptors. *Nature.* 350:505–508.

Lonnbro, P., and I. Wadso. 1991. Effect of dimethyl sulphoxide and some antibiotics on cultured human T lymphoma cells as measured by microcalorimetry. *J. Biochem. Biophys. Methods.* 22:331–336.

Monti, M., P. Hedner, J. Lkomi-Kumm, and S. Valdemarsson. 1987. Erythtocyte thermogenesis in hyperthyroid patients: microcalorimetric investigation of sodium/potassium pump and cell metabolism. *Metabolism.* 36:155–159.

Nishizuka, Y. 1992. Intracellular signaling by hydrolysis of phospholipids and activation of protein kinase C. *Science.* 258:607–614.

Nishizuka, Y. 1995. Protein kinase C and lipid signaling for sustained cellular responses. *FASEB J.* 9:484–496.

Niu, L., W. Vazquez, G. Nagel, T. Friedrich, E. Bamberg, R. E. Oswald, and G. P. Hess. 1996. Rapid chemical kinetic techniques for investigations of neurotransmitter receptors expressed in Xenopus oocytes. *Proc. Natl. Acad. Sci. USA.* 93:12964–12968.

St. Hilaire, P. M., M. K. Boyd, and E. J. Toone. 1994. Interaction of the shiga-like toxin type 1 B-subunit with its carbohydrate receptor. *Biochemistry.* 33:14452–14463.

Tasaki, I., and P. M. Byrne. 1992. Discontinuous volume transitions in ionic gels and their possible involvement in the nerve excitation process. *Biopolymers.* 32:1019–1023.

Tasaki, I., K. Kusano, and P. M. Byrne. 1989. Rapid mechanical and thermal changes in the garfish olfactory nerve associated with a propagated impulse. *Biophys. J.* 55:1033–1040.

Waelbroeck, M., P. Robberecht, P. Chatelain, and P. De-Neef. 1985. Effects of temperature and ethanol on agonist and antagonist binding to rat heart muscarinic receptors in the absence and presence of GTP. *Biochem. J.* 231:469–476.

Wang, Y., and C. Chang-Hwei. 1992. Acetylcholine receptor enriched membrane vesicles in response to ethanol: activity and microcalorimetric studies. *Biophys. Chem.* 43:51–59.

Winston, H., O. J. Marsh, C. K. Suzuki, and C. L. Telk. 1963. Fluorescence of europium thenoyltrifluoroacetonate. I. Evaluation of laser threshold parameters. *J. Chem. Phys.* 39:267–271.

Wintrode, P. L., G. I. Makhatadze, and P. L. Privalov. 1994. Thermodynamics of ubiquitin unfolding. *Protein Struct. Funct. Genet.* 18: 246–253.

Yoshioka, T., and H. Suzuki. 1989. Biophysical aspects of the transmembrane signaling process. *In* Biosignal Transduction Mechanisms. M. Kasai, T. Yoshioka, and H. Suzuki, editors. Japan Scientific Society Press, Tokyo, and Springer Verlag, Berlin. 3–14.